J. Fluid Mech. (1965), *vol.* 23, *part* 2, *pp.* 337–353
Printed in Great Britain

The effect of two-dimensionality on the suppression of thermal turbulence

By J. W. DEARDORFF AND G. E. WILLIS
National Center for Atmospheric Research, Boulder, Colorado

(Received 5 February 1965)

Two-dimensional thermal convection of air between horizontal plates of length much greater than their separation distance is studied numerically by solution of the Boussinesq equations in finite-difference form, and experimentally by constraining motions to lie in a single vertical plane. Rayleigh numbers from 10^5 to 10^7 are employed. Steady rolls with wavelength twice the plate-separation were obtained in both cases. As the experimental two-dimensional constraint is relaxed, short-period turbulent fluctuations in temperature develop, the rolls or cells become only quasi-steady, and their wavelength increases. For the three-dimensional case, very large width-to-height ratios and averaging periods are found necessary before the temperature variance in time approaches the variance in the horizontal.

Introduction

It is of interest in the study of turbulence to determine the importance of three-dimensionality upon the occurrence and structure of the turbulence. It is well known that large differences could be expected between two- and three-dimensional turbulence, since only in two dimensions is the vorticity of fluid elements conserved except for molecular diffusion. Little is known, however, about how necessary three-dimensionality may be in order that turbulent motions occur. Linear stability analyses can shed no light upon the question of whether the unstable motions which may develop will reach steady states, oscillatory or vacillating states, or become irregular in space and time. Theories of turbulence, whether based upon a two-or a three-dimensional framework, assume from the outset that the motions are turbulent. Experimental studies are, as a matter of convenience or desire, three-dimensional, since no effort is usually taken to constrain the motion to two dimensions.

Considerable information is known about two-dimensional convection between horizontal plates, the lower one of which is warmer than the upper. Kuo (1961) has shown that, for Rayleigh numbers up to seven times the critical one for the onset of motion, steady-state rolls or cells which are two-dimensional can exist. However, at these relatively small Rayleigh numbers three-dimensional convection is also believed to be of a steady-state character (Thomas & Townsend 1957).

In a numerical study of two-dimensional convection at a Rayleigh number observed to produce strongly turbulent motions experimentally, it was shown

by Deardorff (1964) that the convective motions are essentially steady and non-turbulent. However, it was not known if the absence of turbulent motions was associated with the two-dimensional assumption or with the limited width employed (only twice the height).

The present study was motivated in particular by the desire to determine which of these two factors caused the motions to be non-turbulent. The previous study is here extended to a region of length eight times the plate separation, and an experimental study is also conducted in which motions are constrained to lie in a vertical plane.

In § 1 a direct numerical method is used, rather than a more theoretical analytic method, in order to avoid assumptions about the non-linear terms of the equations, and in order to be able to treat the equivalent of a large number of Fourier components of the motion in both the horizontal and the vertical directions.

1. Numerical study

1.1. *Two-dimensional theory*

The Boussinesq approximation of constant density, except in the buoyancy term of the vertical equation of motion, is employed, as well as the two-dimensional assumption. The vorticity and thermal diffusion equations are made non-dimensional by division of all lengths by h, the plate separation; all velocities by ν/h, where ν is the kinematic viscosity; time by h^2/ν; and temperature by ΔT, the positive temperature difference between horizontal plates. The equations then become, respectively,

$$\frac{\partial \eta}{\partial t} + u\frac{\partial \eta}{\partial x} + w\frac{\partial \eta}{\partial z} = \frac{Ra}{Pr}\frac{\partial T}{\partial x} + \left(\frac{\partial^2}{\partial x^2} + \frac{\partial^2}{\partial z^2}\right)\eta, \tag{1}$$

and

$$\frac{\partial T}{\partial t} + u\frac{\partial T}{\partial x} + w\frac{\partial T}{\partial z} = \frac{1}{Pr}\left(\frac{\partial^2}{\partial x^2} + \frac{\partial^2}{\partial z^2}\right)T. \tag{2}$$

In these non-dimensional equations the vorticity is given by $\eta \equiv \partial w/\partial x - \partial u/\partial z$; u and w are the respective non-dimensional velocity components in the horizontal x- and vertical z-directions; Ra is the Rayleigh number $g\Delta T h^3/\overline{T}\nu k$, where g is the gravitational acceleration, $\overline{T}$ is the mean temperature of the gas, and k is the thermal diffusivity; T is the non-dimensional temperature; and Pr is the Prandtl number ν/k. The use of non-dimensional quantities will be retained throughout the paper.

A stream function ψ may be defined by

$$u = -\partial\psi/\partial z, \quad w = \partial\psi/\partial x, \tag{3}$$

so that the simplified continuity equation

$$\partial u/\partial x + \partial w/\partial z = 0 \tag{4}$$

is satisfied. The vorticity then becomes

$$\eta = \partial^2\psi/\partial x^2 + \partial^2\psi/\partial z^2. \tag{5}$$

Equations (1), (2), (3) and (5) were expressed in finite-difference form, and applied at 80 points horizontally and 40 points vertically into which the region between plates was subdivided. A length of eight times the height was obtained by allowing the horizontal grid increment Δx, to be four times larger than the vertical grid increment Δz. A Rayleigh number of $6{\cdot}75 \times 10^5$ and Prandtl number of 0·71 (appropriate to air) were specified, with boundary conditions of constant temperatures and no fluid motion at the horizontal plates. The vorticity at the horizontal boundary, η_0, was related to the stream function at a point Δz interior to the boundary through a truncated Taylor expansion as follows:

$$\psi(0+\Delta z) = \psi(0) + (\partial\psi/\partial z)_0 \Delta z + \tfrac{1}{2}(\partial^2\psi/\partial z^2)_0 (\Delta z)^2. \tag{6}$$

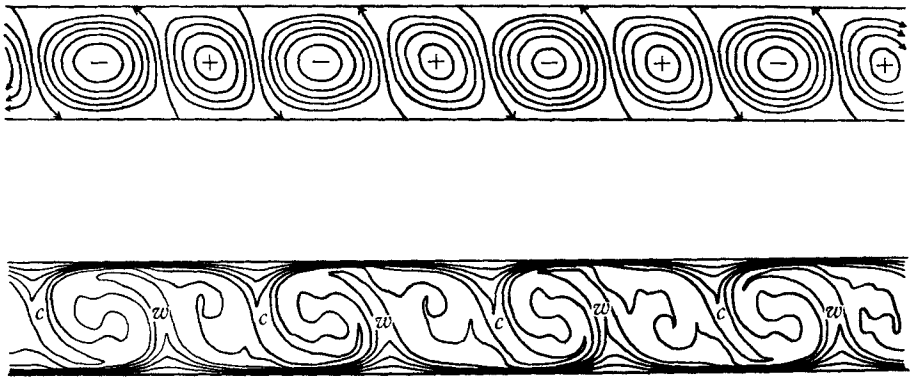

FIGURE 1. Streamlines (upper half) and isotherms (lower) at $t = 0{\cdot}22$. Streamlines are at intervals of 20, with the zero value intersecting boundaries. Isotherms are at intervals of 0·1. Warm and cool plumes are labelled w and c respectively.

Then $\eta_0 = (\partial^2\psi/\partial z^2)_0$ is found to be

$$\eta_0 = 2\psi(0+\Delta z)/(\Delta z)^2, \tag{7}$$

since $\psi(0) = 0 = (\partial\psi/\partial z)_0$ because of the conditions $u_0 = w_0 = 0$. Cyclic conditions were used at the end walls. Initial conditions were zero motion and a sinusoidal temperature perturbation superimposed upon a linear decrease of temperature from the lower plate to the upper plate. Calculations were made on a CDC 3600 digital computer. Other details of the calculation are the same as for case (c) of Deardorff (1964).

1.2. *Numerical results*

After a non-dimensional time of 0·04 had elapsed it was evident that the motions were approaching a steady state, except for an oscillation which became established at $t = 0{\cdot}10$ and persisted until calculations were terminated at $t = 0{\cdot}22$. The streamlines and isotherms at this later time are shown in figure 1. There are eight vortices present, so that the preferred non-dimensional wavelength in the horizontal direction is $2(1 \pm \frac{1}{8})$. The uncertainty of 12·5 % reflects the fact that an even number of vortices was forced by the cyclic end conditions. It is interesting to note that stability studies for the much smaller, critical Rayleigh

number of 1708 yield a two-dimensional wavelength of 2·02 (Chandrasekhar 1961).

The non-dimensional boundary heat flux, or Nusselt number, is shown as a function of time in figure 2. It starts out with the molecular value of unity and soon overshoots the equilibrium value which is seen to be about 7·8 for small oscillations, and 7·2 for larger oscillations. The upper dashed line is the empirical value obtained from experiments of Silveston (1958), and the lower one that of Globe & Dropkin (1958) for the same Rayleigh and Prandtl numbers.

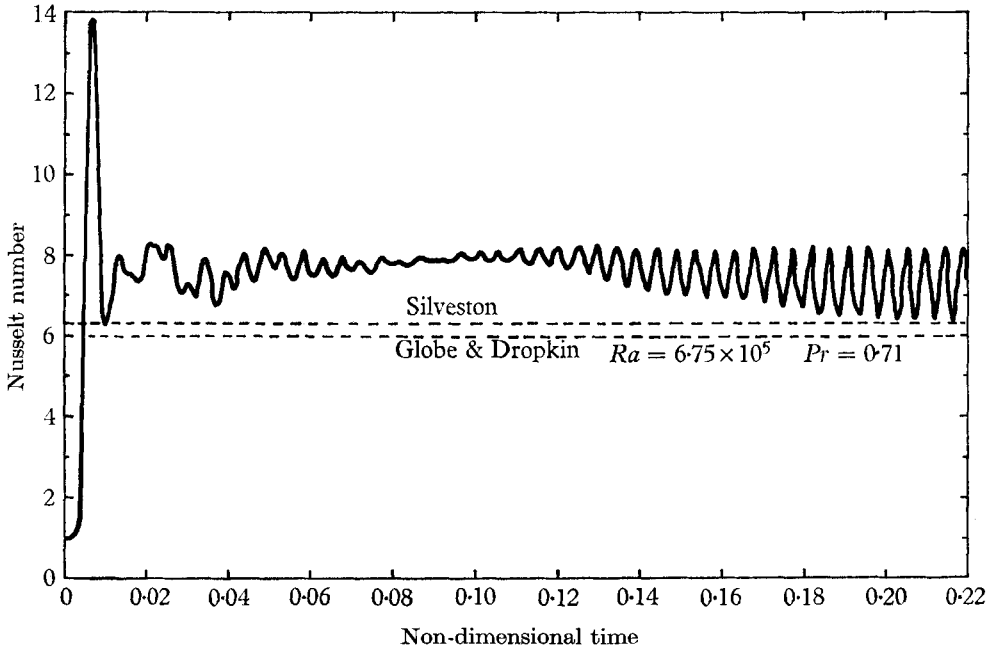

FIGURE 2. Nusselt number as a function of time.

The oscillation is associated with unequal intensities of adjacent vortices and with organized inclination or swaying of the thermal plumes (figure 1). It is quite evident that the organized inclination of the plumes and cell-boundaries could not occur if solid rather than cyclic end boundaries were employed. The oscillation definitely appears to be real and not caused by any numerical instability, because nearly 400 time steps were required for each cycle of the oscillation. It is not clear, however, if this kind of oscillation would always occur independent of the choice of initial conditions, or whether its occurrence requires the proper kind of perturbation to persist after the steady-state configuration has been approached. Once established, however, the oscillation appears to maintain itself in the following manner. The alternating vortices which are more intense and wider than their neighbours gradually cause, by advection, the warm and cool plumes at their peripheries to become farther apart. (At the same time, the plumes become tilted in the direction of circulation of the more intense vortices.) The less intense vortices then find the horizontal temperature gradient

across their widths to be of greater magnitude than that across the larger vortices. At this time the vorticity in the small vortices must begin to increase in magnitude, while that of the larger vortices must decrease in magnitude, because of the buoyancy term in equation (1). At a later time when all vortices are of equal intensity, the thermal plumes have not yet become evenly spaced but continue to cause the growing vortices to become more intense. The cycle starts to reverse at the moment when the warm and cool plumes become evenly spaced. At time $t = 0{\cdot}22$, for which figure 1 applies, the plumes are in the stage of increasing their tilt, and the more intense negative vortices are still amplifying. The oscillations gradually increase in amplitude as the motions in alternate vortices become more exactly in phase.

At a non-dimensional time of 0·09 before the well-organized oscillations had become initiated, the Nusselt number reached a maximum value of 7·8 in conjunction with the fact that the plumes were then directed vertically and thermal boundary layers were most compressed. The later decrease of the average Nusselt number as the oscillation slowly increased reflects the fact that the plumes were then usually inclined. These results suggest how turbulence in three-dimensional convection causes the Nusselt number to be somewhat smaller than the two-dimensional value through the disruptive effect upon the major thermal plumes.

The main conclusions to be drawn from these two-dimensional calculations are that two-dimensionality prevents the occurrence of irregular, turbulent convection, at least for Rayleigh numbers up to $6{\cdot}75 \times 10^5$, and that the preferred wavelength of two-dimensional cells at this Rayleigh number is still about the same as at the critical Rayleigh number. Both conclusions strengthen the previous findings of Deardorff (1964). However, the latter conclusion does not agree well with results of a quasi-linear study by Herring (1964) in which a non-dimensional wavelength of about 0·5 yielded maximum heat flux at this Rayleigh number, though at a very large Prandtl number.

In the next section, experimental results will be given of the absence of turbulent motions for convection constrained to be two-dimensional, for three different Rayleigh numbers spanning that of the numerical study. In addition, the manner in which wavelengths and intensities of temperature variations change as the experimental two-dimensional constraint is relaxed will be examined.

2. Experimental study

2.1. *Basic equipment*

A schematic drawing of the convection chamber is shown in figure 3. The height h is adjustable between 5 and 20 cm, and the temperature difference ΔT is typically between 15 and 30 °C. Rather large values of ΔT are desirable for accuracy of temperature measurements, but values larger than about 30 °C cause undesirably large vertical variation of ν and k, in contrast to their assumed constancy in the Boussinesq approximation. The shaded barriers in the figure, when placed rather close together, constitute the constraint which causes motions between them to be parallel to the barriers. They are made of Styrofoam of 5 cm

thickness, and extend the entire length and height of the chamber. This material was chosen because of its good insulation and small heat capacity.

The horizontal plates of the chamber are aluminium of 1·3 cm thickness, and have smooth surfaces. They are maintained at two different temperatures by circulation of heated and refrigerated water through small aluminium channels immediately exterior to the lower and upper aluminium plates, respectively. The entire system is insulated with fibreglass of 5 cm thickness, except for the outer lateral walls of the chamber which consist of Plexiglass of 1·3 cm thickness. A given temperature difference ΔT, as measured by thermocouples within the circulating water, can be maintained constant within about $\pm$ 0·3 °C over a period of several days.

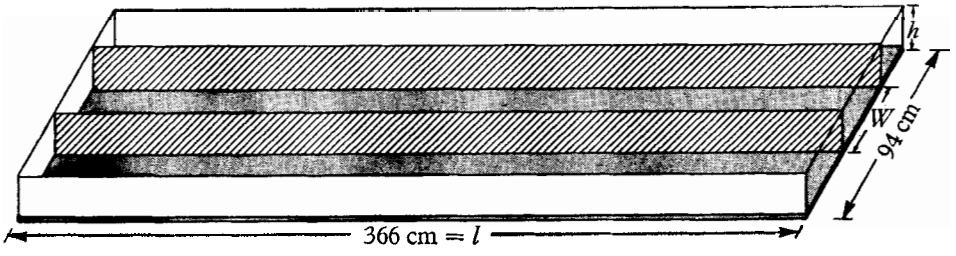

Convection chamber

FIGURE 3. Schematic drawing of convection chamber as viewed from one side and from above.

In determining the Rayleigh number for these experiments the minute temperature drop across the aluminium plate could safely be neglected in comparison with ΔT. The greatest uncertainty in Ra was due to uncertainty in ν and k stemming from uncertainty of the air density. The latter quantity was computed from the perfect gas law assuming a pressure of 850 millibars. The actual pressure may have differed by $\pm$ 3 % from this figure, and Ra may have been in error by $\pm$ 6 %.

Measurements of air temperature between the barriers were taken by thermocouples with time constants of about 0·5 sec.

2.2. *Cell wavelength*

Temperature measurements were taken midway between barriers and horizontal plates, both at a fixed point for a period of 1 h, and along the entire length of the chamber over an interval of about 2 min. From records of the latter, steady or quasi-steady cell-like structures were observed along the length of the chamber, and their number could easily be counted when the barrier separation W was small or comparable with h. Even at larger barrier separations, when turbulence was well developed, the number of predominant cycles could still be determined, as from figure 4, though with some subjective and sampling errors. These errors could not have been appreciable, however, for a horizontal spectrum of temperature to be discussed later (figure 6) showed a very strong peak corresponding to the same wavelength as that obtained subjectively. The average dominant wave-

length was determined as the length of the chamber l, divided by the number of predominant cycles.

For simplicity, the cyclic structures will here be called 'cells', although their horizontal plan form was not directly observed. For small aspect ratios (W/h),

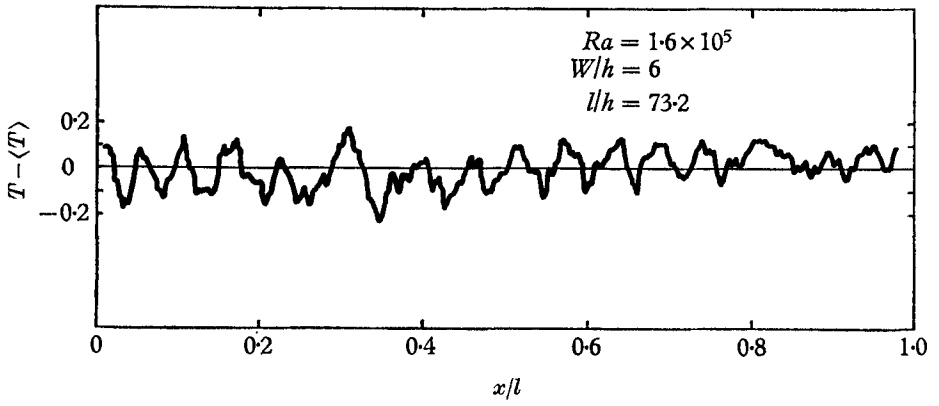

FIGURE 4. A record of temperature against longitudinal distance within the convection chamber.

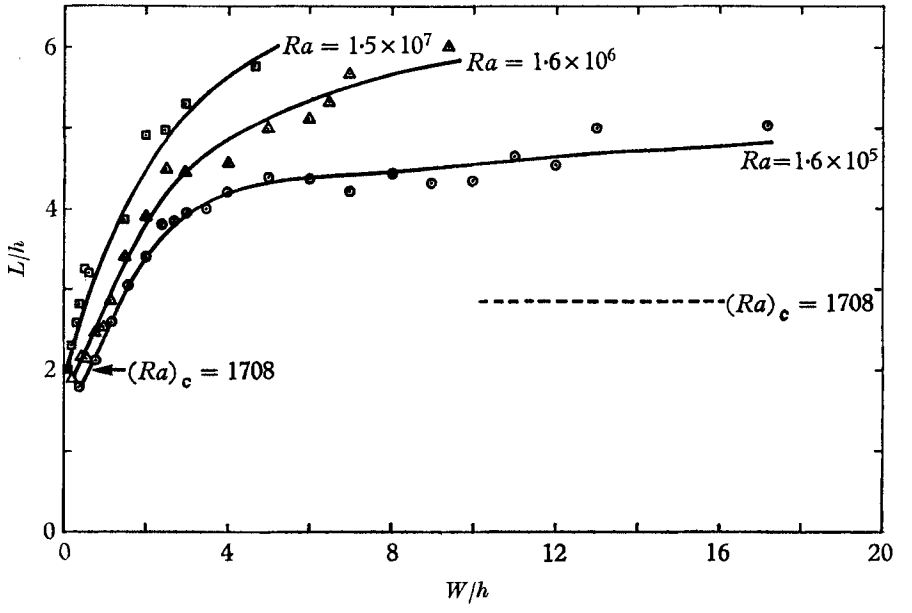

FIGURE 5. Non-dimensional cell wavelength L/h against aspect ratio W/h for three Rayleigh numbers. W is the width between barriers, and h is the separation between horizontal plates.

however, the structures are known from temperature measurements to have the appearance of rolls lying in a vertical plane between barriers. At aspect ratios in the vicinity of 2 or 3 the structures became three-dimensional, and the term 'cell' is more appropriate.

The non-dimensional wavelength L/h is shown as a function of aspect ratio W/h and of Ra in figure 5. At small values of W/h, L/h has a value slightly less than 2, and agrees rather well with the numerically calculated value reported in § 1. As W/h increases the motions become increasingly three-dimensional, and L/h increases. The arrow and dashed line in figure 5 refer to the two- and three-dimensional values, respectively, of L/h when Ra has the critical value, $(Ra)_c$, of 1708. At much larger Rayleigh numbers L/h is seen to become increasingly larger than the critical three-dimensional value, and appears to approach asymptotic values for $W/h > 15$.

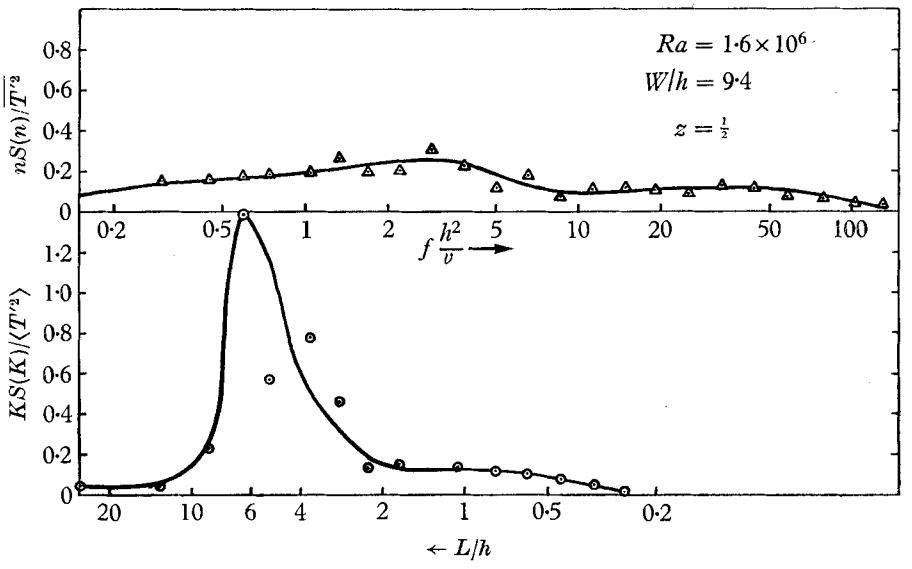

FIGURE 6. Normalized power spectrum of temperature at $z = \frac{1}{2}$ at a fixed point (upper curve), and with respect to longitudinal co-ordinate (lower curve).

The quasi-stationarity of the predominant cells at super-critical Rayleigh numbers, and the increase of L/h with Ra for large values of W/h, seem to be consistent with satellite photographs of large-scale atmospheric cellular structures with $L/h \simeq 30$ (Krueger & Fritz 1961). However, the comparison is not close because of the effect of the Earth's rotation tending to increase $(Ra)_c$ and to decrease L/h (Nakagawa & Frenzen 1955), and because of the presence of wind shear, water vapour, and vertical decrease of density in the atmosphere. Also, the atmospheric Rayleigh numbers, though possibly very large, can hardly be estimated because of uncertainty of surface and inversion temperatures.

The longitudinal aspect ratio (chamber length divided by h) limits the number of cells present for any given W/h and Ra. Table 1 gives values of longitudinal aspect ratio for the three Rayleigh numbers employed, as well as other pertinent information. Reference to table 1 and figure 5 indicates there were 6 cells, or 12 vortices, present in the longitudinal direction for $Ra = 1{\cdot}6 \times 10^6$ and $W/h > 9$. An increase of Ra, with h held constant, leads to an increase of L/h; but since a small integral number of vortices must be present, the predominant cell length

changes in discrete steps. It appears likely that in any actual experiment the discrete increases of predominant cell length which occur if Ra is increased would be associated with small but discrete changes of heat flux and other properties of the convection. In the experimental study of Malkus (1954*a*), discrete changes in the slope of the heat-flux versus ΔT, or Rayleigh number, curve were observed for constant aspect ratio. It seems unlikely, however, that these changes were associated with discrete changes in predominant cell diameter; for the ratio of chamber diameter to height utilized by Malkus was as small as 2·5 and yet discrete slope transitions were observed at $Ra = 8{\cdot}5 \times 10^5$ and $1{\cdot}6 \times 10^6$. Inspection of figure 5 suggests that for this small aspect ratio in both horizontal directions, only one dominant cell or half-cell would be present at *any* large Rayleigh number.

Ra	ΔT (°C)	h (cm)	$\bar{\bar{T}}$ (°K)	ν	k (cm²/sec)	Longitudinal aspect ratio
$1{\cdot}6 \times 10^5$	17·1	5·1	293	0·182	0·255	73·2
$1{\cdot}6 \times 10^6$	22·8	10·2	300	0·187	0·262	36·6
$1{\cdot}5 \times 10^7$	28·7	20·4	304	0·192	0·269	18·3

TABLE 1

Normalized power spectra of temperature measured at a fixed point, and also longitudinally within the convection chamber, are shown in figure 6 for $Ra = 1{\cdot}6 \times 10^6$. The spectral estimates, denoted by S, were obtained by direct Fourier analyses of the original records (digitized for equally spaced intervals of 1 sec and 1 cm, respectively) and subsequent averaging of one-half the sum of the squared Fourier sine and cosine coefficients over neighbouring frequencies or wave-numbers. It was evident from the original continuous records that negligible intensity resided in periods or wavelengths shorter than the data intervals utilized, this minimizing any possible effects of aliasing. The upper ordinate $nS(n)/\overline{T'^2}$ is the fraction of the temporal variance per increment of the logarithm of the Fourier-component number n, where $\overline{T'^2}$ is the temporal variance evaluated for a one-hour period. For convenience the abscissa has been converted to non-dimensional frequency fh^2/ν, where f, the frequency in cycles per second, equals $n/3600\,\mathrm{sec}^{-1}$. The lower ordinate $KS(K)/\langle T'^2\rangle$ is the fraction of the longitudinal variance per increment of the logarithm of the Fourier wave-number K, where $\langle T'^2\rangle$ is the longitudinal variance evaluated over 260 cm, a distance somewhat less than the chamber length. For convenience the abscissa of the lower spectrum has been converted to L/h, where $L = 260/K$ cm. Temperatures for the lower spectrum of the figure were obtained by passage of a platinum resistance wire of $1{\cdot}3\,\mu$ diameter and 1·5 mm length along the convection chamber at a uniform speed of 26 cm sec^{-1}, and this spectrum is an average from four such runs for $0{\cdot}4 < z < 0{\cdot}6$, and with $W/h = 9{\cdot}4$. The strong peak at $L/h = 6$ agrees with the value which can be obtained from figure 5. The flatness of the

upper spectrum, in contrast, indicates that the predominant cells do not shift position or phase with any preferred frequency for large aspect ratios.

Friction and conduction at the lateral barriers is an undesired effect, in comparing these experiments with the numerical calculations. However, these factors did not appear to influence appreciably values of L/h, which continued to increase smoothly upwards from about 2 as W/h increased.

2.3. *Temperature variance*

The non-dimensional temperature variance associated with variations along the length of the chamber midway between plates and barriers, is given in figure 7 as a function of W/h and Ra. The rapid decrease of $\langle T'^2 \rangle$ as W/h first increases

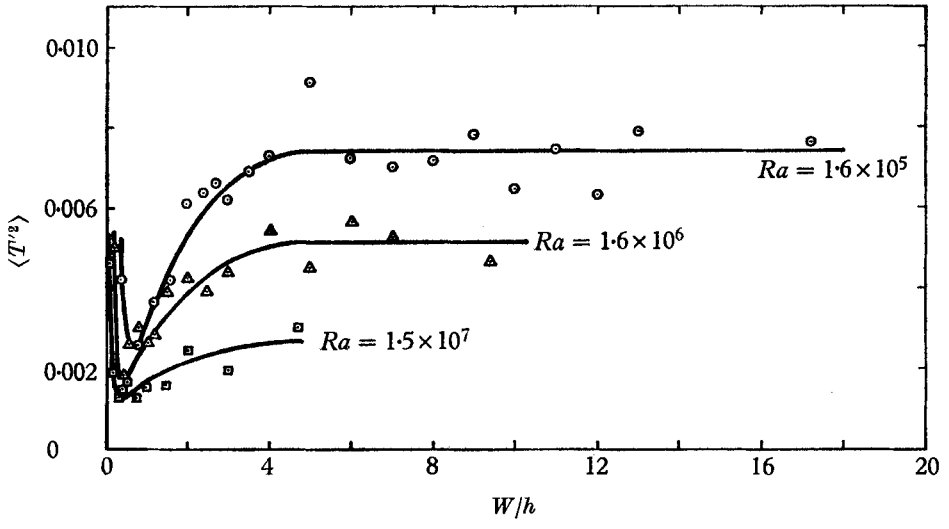

FIGURE 7. Non-dimensional longitudinal temperature variance $\langle T'^2 \rangle$ against aspect ratio W/h for three Rayleigh numbers.

from zero occurs because of relaxation of the strong effect of lateral friction upon the motions. For when speeds are quite small but finite, a (warm) thermal plume does not mushroom far outwards upon reaching the opposite (cool) plate, and thus cannot appreciably reduce the intensity of its neighbouring (cool) plumes. Then all the plumes are more intense, with respect to ΔT, than when motions are stronger and when plumes may wrap halfway or more around a vortex as in figure 1. Since the intensity of the motions increases with Ra, the same reasoning can also qualitatively explain the decrease of $\langle T'^2 \rangle$ with increasing Ra.

The increase of $\langle T'^2 \rangle$ with aspect ratio, for $W/h > 1$, is closely associated with the increase of L/h with aspect ratio. As the major thermal plumes become spaced farther apart, it appears reasonable that a given plume would find it more difficult to maintain its previous intensity upon mushrooming farther horizontally, and would then interfere less with the development of its neighbouring plumes. Thus the increase of $\langle T'^2 \rangle$ and L/h together is quite consistent.

The value of $\langle T'^2 \rangle$ at $z = \frac{1}{2}$, obtained from the two-dimensional calculations of § 1, is 50 % larger than the minimum for that Rayleigh number which can be estimated from figure 7. The discrepancy may be caused by thermal conduction at the lateral walls. The thermal conductivity of the Styrofoam barriers is 50 % larger than that of still air, so that they are undesirably effective in diffusing temperature fluctuations at their inner surfaces both vertically and laterally outwards. In a much cruder experimental study of two-dimensional convection (Deardorff 1964) in which the lateral insulation was poorer than in the present study, $\langle T'^2 \rangle$ at $z = \frac{1}{2}$ was only 0·0016 for $Ra = 5{\cdot}5 \times 10^5$. It is thus suggested here that the effect of lateral friction in increasing $\langle T'^2 \rangle$ predominated over the modifying effect of lateral conduction for $W/h \lesssim 0{\cdot}1$, and vice versa for $W/h \gtrsim 0{\cdot}1$. Both effects were probably negligible for $W/h > 1$.

At this point a qualitative explanation may be offered for the increase of predominant wavelength with aspect ratio. The thermal variance equation will be utilized, as it contains fewer unknown terms than does the turbulent kinetic-energy equation. If the fluctuating part of equation (2) is multiplied by T' and averaged horizontally, the equation

$$\langle wT' \rangle \frac{\partial \langle T \rangle}{\partial z} + \frac{\partial}{\partial z} \tfrac{1}{2} \langle wT'^2 \rangle = \frac{1}{Pr} \left[\frac{\partial^2}{\partial z^2} \tfrac{1}{2} \langle T'^2 \rangle - \left\langle \frac{\partial T'}{\partial x_i} \frac{\partial T'}{\partial x_i} \right\rangle \right] \quad (i = 1, 2, 3) \tag{8}$$

is obtained for the statistically steady state. Now at $z = \frac{1}{2}$ the source term $\langle wT' \rangle \partial \langle T \rangle / \partial z$ is negligible because of the isothermal lapse rate (Deardorff 1964), and the term $\partial^2 \frac{1}{2} \langle T'^2 \rangle / \partial z^2$ is negligible because of the near constancy of $\langle T'^2 \rangle$ in the central region. Thus at $z = \frac{1}{2}$,

$$\frac{\partial}{\partial z} \tfrac{1}{2} \langle wT'^2 \rangle \simeq -\frac{1}{Pr} \left\langle \frac{\partial T'}{\partial x_i} \frac{\partial T'}{\partial x_i} \right\rangle. \tag{9}$$

The right-hand side of (9) may be regarded as a 'thermal dissipation', and when an increasing aspect ratio allows small-scale turbulence to appear, both sides of (9) must increase in magnitude. The left-hand side of (9) could most easily increase in magnitude if the intensity T'^2 of the dominant thermal plumes were to increase. Since an increase of $\langle T'^2 \rangle$ has already been seen to be associated with an increase of wavelength of the large cells, an increase of L/h with increasing small-scale turbulence and aspect ratio thus follows from this chain of reasoning. The reason for the term $\partial \frac{1}{2} \langle wT'^2 \rangle / \partial z$ being negative at mid-level and being associated with the major plumes was given by Deardorff (1964).

The measured decrease of $\langle T'^2 \rangle$ with increasing Rayleigh number, only qualitatively explained earlier, can be compared quantitatively with the theory of Malkus (1954*b*). Malkus's equation for the non-dimensional temperature variance may be written

$$\langle \langle T'^2 \rangle \rangle = 2 \ln Nu / 3\pi^2 Nu, \tag{10}$$

where $\langle \langle T'^2 \rangle \rangle$ is the variance averaged over all space. Comparison of $\langle T'^2 \rangle$ measured at $z = \frac{1}{2}$ with equation (10) was accomplished after obtaining an average of $\langle T'^2 \rangle$ over z by use of data collected with the platinum resistance wire

for $Ra = 1{\cdot}6 \times 10^6$. The Nusselt number Nu was obtained from equation (11). It was found that

$$\langle\langle T'^2\rangle\rangle \cong 1{\cdot}85\langle T'^2\rangle_{z=\frac{1}{2}}.$$

While equation (10) correctly predicts the decrease of $\langle\langle T'^2\rangle\rangle$ with Ra, the predicted values of $\langle\langle T'^2\rangle\rangle$ are about 1·9 times larger than the observed values. The results for $W/h > 6$ are tabulated in table 2. In a similar comparison by Thomas & Townsend (1957), Malkus's predicted values were found to be too large by a factor of 2·6. The discrepancy between the two *experimental* results is caused by the underestimation of the time variance, as was measured by Thomas & Townsend, in comparison with the horizontal variance unless an extremely large averaging period and aspect ratio is used. In the experiment of Thomas & Townsend with an aspect ratio of about 6 and with $Ra = 6{\cdot}75 \times 10^5$, a quasi-steady cell was believed to be present. This belief is supported by our results of quasi-steady cells at even larger aspect ratios. The discrepancy between the theoretical and observed values in table 2 could be caused by one or more of the several assumptions made in Malkus's theory.

Ra	$\langle\langle T'^2\rangle\rangle$ Malkus's theory	$\langle\langle T'^2\rangle\rangle$ observed
$1{\cdot}6 \times 10^5$	0·0240	0·0137
$1{\cdot}6 \times 10^6$	0·0178	0·0096
$1{\cdot}5 \times 10^7$	0·0114	0·0055

TABLE 2

2.4. *Degree of turbulence*

If the motions were fully turbulent, the temperature variance measured at a fixed point, $\overline{T'^2}$, could be assumed identical to the horizontal variance, $\langle T'^2\rangle$, for a sufficiently long averaging period. Therefore, a 'degree of turbulence', R, as evidenced by measurements at $z = \frac{1}{2}$, may be conveniently defined as

$$R \equiv \overline{T'^2}/\langle T'^2\rangle.$$

For steady cellular motion $R = 0$. For three-dimensional flow this case presumably occurs for $1708 < Ra < 30{,}000$; for at the higher Rayleigh number the Nusselt-number against Rayleigh-number curve changes slope from the laminar value of $\frac{1}{4}$ to a value of about $\frac{1}{3}$ (Silveston 1958), characteristic of turbulent flow for which $R = 1$, presumably. Of course, this definition of R would treat a simple oscillation of the cells as turbulence whereas only the disorganized motions are usually regarded as being turbulent. However, periodic fluctuations of temperature were only observed at the smallest Rayleigh number studied and for very small aspect ratios. Values of R, measured for an averaging period of 1 h, are shown in figure 8. The large amount of scatter was caused mainly by the insufficiency of an hour's averaging period. The temporal variance is crucially dependent upon the amount of phase shift of the predominant cells; sometimes these cells would shift phase during the averaging period, and sometimes not. Values of $R > 1$ were presumably associated with the sampling error of $\langle T'^2\rangle$.

The slow increase of R for $0 < W/h < 1$ is mainly due to an increase in intensity of short-period non-cellular motions, while the more rapid increase for $1 < W/h < 3$ is associated largely with increasing phase shift and distortions of the dominant cells. This behaviour is consistent with the dimensional power spectra of figure 9 calculated by direct Fourier analyses. For convenience $nS(n)$ is here plotted logarithmically although the property of equal variance for equal

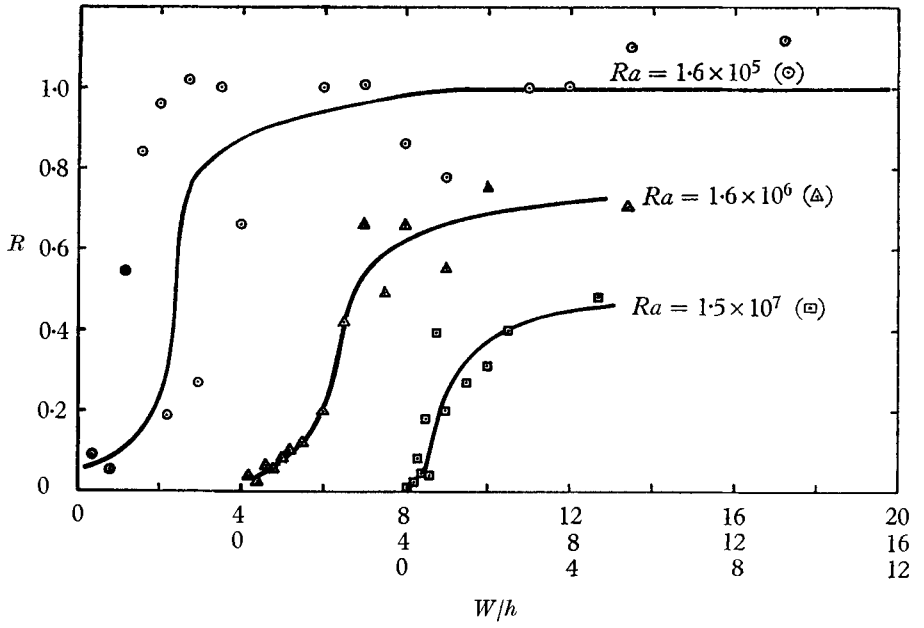

FIGURE 8. Degree of turbulence R against aspect ratio W/h for three Rayleigh numbers. Note shift of origin of successive curves four units to the right.

area is not preserved. For $W/h = 0{\cdot}4$ there is relatively little intensity at the shorter periods, but after W/h has reached 1·5 most of the variance is caused by fluctuations of period less than a minute. For $W/h = 9{\cdot}4$ significant power resides in much longer-period fluctuations which must be associated with slow shifts in position of the major cells. For the large aspect ratios an appreciable fraction of the total temporal variance appears to have been cut off by the finite averaging for $Ra = 1{\cdot}6 \times 10^6$ and larger.

The curves of R in figure 8 all presumably approach unity as $W/h \to \infty$. However, at the larger Rayleigh numbers they approach unity very slowly. This result is probably associated with increasing steadiness of the predominant cells as the Rayleigh number increases and the cells become longer. A much larger averaging period than 1 h may then be necessary before the temporal variance attains its full value. The increased steadiness of the predominant cells, as the Rayleigh number is increased, may also be aided by the decreasing longitudinal aspect ratio of the convection chamber (see table 1).

For the smallest Rayleigh number studied periodic fluctuations of long period were observed for $W/h = 0{\cdot}4$, and vacillating fluctuations for $W/h = 0{\cdot}8$. An

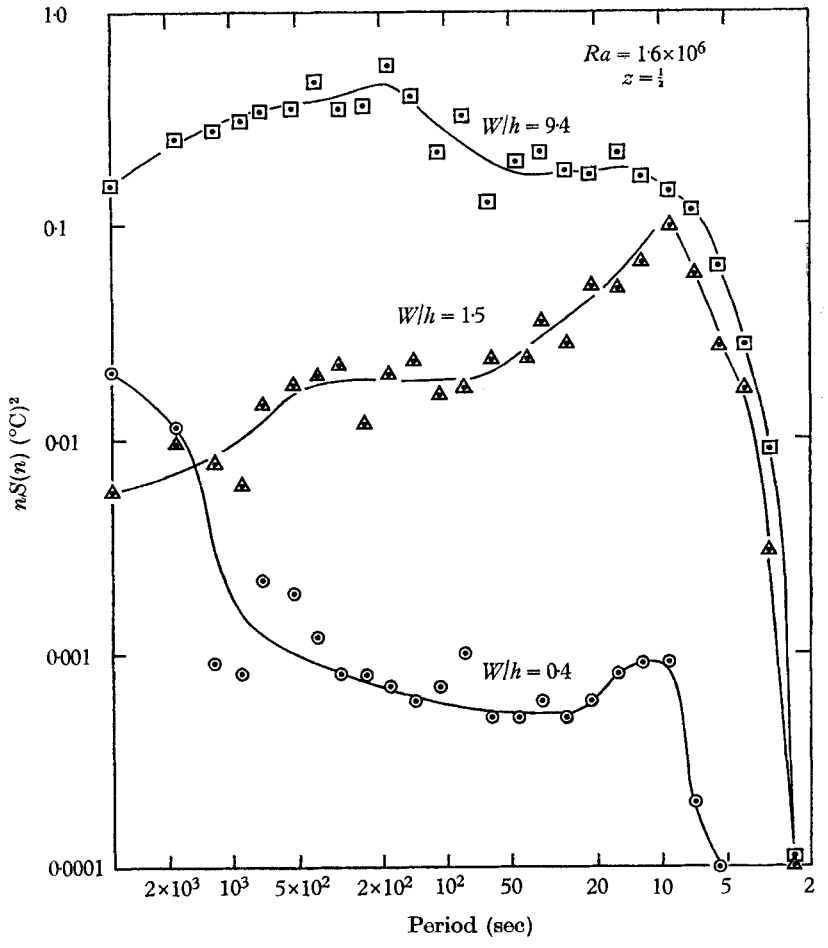

FIGURE 9. Dimensional power spectra of temperature measured at a fixed point for three aspect ratios, and for $Ra = 1{\cdot}6 \times 10^6$.

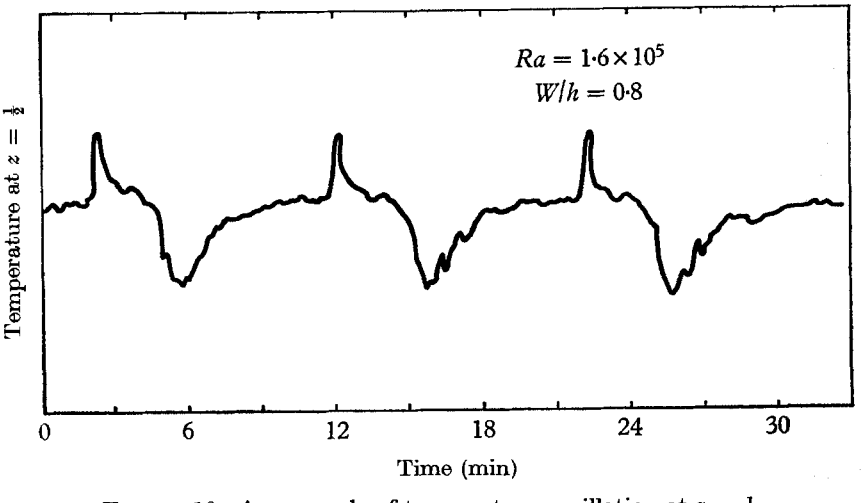

FIGURE 10. An example of temperature vacillation at $z = \frac{1}{2}$.

interesting example of the vacillation is shown in figure 10. The pattern which repeats with a period of about 10 min is asymmetrical, and temperatures measured simultaneously at a point 1·8 m distant showed an entirely different pattern of vacillation to be occurring. The smallest scale features of the vacillation do not repeat. For larger values of W/h vacillation did not occur, and the fluctuations which did occur were turbulent in the usual sense.

Since periodic or vacillating fluctuations are too regular to be considered turbulent, their influence upon R in figure 8 was eliminated for $W/h = 0{\cdot}4$ and $0{\cdot}8$, and $Ra = 1{\cdot}6 \times 10^5$. This could be done approximately, for these two cases, upon examination of the time spectra which naturally showed sharp peaks in intensity at the periods of the oscillation and vacillation. These peaks were simply levelled off before calculation of $\overline{T'^2}$ and R.

2.5. *Nusselt number*

The non-dimensional heat flux, or Nusselt number Nu, was obtained from the temperature difference between two nickel resistance wires located 1 and 2 mm, respectively, above the bottom plate, and extending the entire length of the

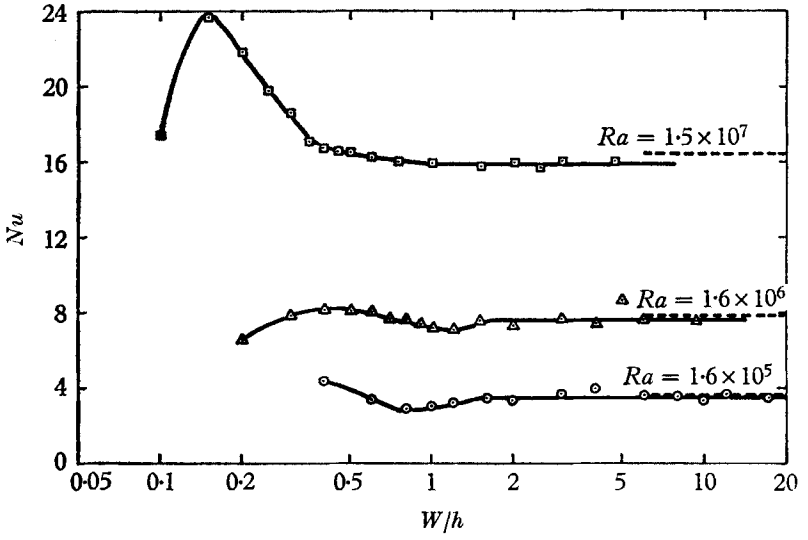

FIGURE 11. Nusselt number Nu against aspect ratio for three Rayleigh numbers.

chamber. It was found that the linear boundary gradient extended at least 2 mm from the plate. The wires, of diameter 0·08 mm, were calibrated by producing constant and easily measured *stable* temperature gradients within the chamber. Individual measurements of Nu shown in figure 11 are values averaged over 1 min periods. This small averaging period here was sufficient because of the large length of the resistance wires. For $W/h > 2$ the Nusselt numbers are essentially independent of aspect ratio and agree well with the dashed lines on the right, which were calculated from the empirical formula of Globe & Dropkin:

$$Nu = 0{\cdot}069(Ra)^{\frac{1}{3}}(Pr)^{0{\cdot}074}. \tag{11}$$

This lack of dependence of Nu upon W/h has only cursorily been examined before by Malkus (1954*a*) and Globe & Dropkin (1958).

At extremely small values of W/h, figure 11 indicates that Nu is smaller than the large-width value, undoubtedly because of the effect of lateral friction. However, at slightly larger values of W/h of about 0·4, Nu has a maximum followed by a slight secondary minimum. We believe that the maximum reflects the efficiency of the steady convective regime in transporting heat, in agreement with the larger value of Nu calculated in § 1 for the two-dimensional case. If the earlier arguments concerning the effect of lateral heat transfer upon $\langle T'^2 \rangle$ are correct, the maxima of these Nu curves would be expected to be even greater if the lateral insulation had been better.

The change of intensity of the heat-flux maximum with Rayleigh number, and the occurrence of the secondary minimum at the smaller Rayleigh numbers are unexplained features of figure 11.

The approximate constancy of Nusselt number with aspect ratio for $W/h > 2$, even though $\langle T'^2 \rangle$ increases strongly from $1 < W/h < 4$, is another indication of the compensatory nature of the vertical velocity and temperature variances at mid-level. That is, if $\langle w^2 \rangle$ is caused to decrease for some reason, the plumes then become less extended so that $\langle T'^2 \rangle$ increases; while $\langle wT' \rangle$, which at $z = \frac{1}{2}$ essentially equals Nu, tends to remain constant if the correlation between w and T' tends to remain constant.

2.6. *Conclusions*

The most important conclusion of this study is that two-dimensional parallel-plate convection in a vertical plane has the form of rolls which are non-turbulent in character, at least for air with Rayleigh numbers up to 10^7. This conclusion was obtained both experimentally and theoretically. The numerically derived two-dimensional heat flux was found to be 25% greater than the three-dimensional experimental value, and values of the two-dimensional heat flux obtained in the laboratory also tended to be larger than the three-dimensional value. Apparently the presence of aperiodic turbulent motions has a disorganizing effect upon the major thermal plumes, and brings about a somewhat smaller heat flux than for the steady (two-dimensional) convection at the same Rayleigh number.

As the experimental two-dimensional constraint is relaxed, short-period turbulent motions appear, and the large-scale rolls or cells are able to shift somewhat and change shape. At the same time, the wavelength of these rolls increases gradually from the critical two-dimensional value, and the horizontal temperature variance also increases gradually. Because of complicating effects of lateral friction and thermal conduction, no definite two-dimensional value could be measured for the horizontal temperature variance. The heat flux, in contrast to the predominant cell length and temperature variance, quickly approaches a constant three-dimensional value as the aspect ratio becomes larger than one.

The 'degree of turbulence', R, increases most rapidly with aspect ratio for aspect ratios between 1 and 3. Thus it may be roughly stated that for aspect

ratios less than 2 the convection is mainly non-turbulent, and for aspect ratios greater than 2 it is mainly turbulent with respect to time. Surprisingly large horizontal aspect ratios, and averaging period, are required at large Rayleigh numbers, however, before the temperature variance in time approaches that in the horizontal. For $Ra > 10^6$ our results suggest that for approximate equality of the two averages, horizontal aspect ratios should be larger than about 20, and averaging periods greater than one hour (non-dimensional period greater than 200). The severity of these criteria increases with increasing Rayleigh number.

The dimensions of the convection chamber were not large enough to establish beyond doubt whether or not the presence of predominate cells of large wavelength, at large Rayleigh numbers, is characteristic of the horizontally infinite case. However the presence of quasi-steady cells with very large aspect ratios for $Ra = 1{\cdot}6 \times 10^5$, and the tendency for the cell length to become independent of aspect ratio for $Ra = 1{\cdot}6 \times 10^6$, suggest that quasi-steady cells of distinct size do exist for very large horizontal extent at large Rayleigh numbers.

REFERENCES

CHANDRASEKHAR, S. 1961 *Hydrodynamic and Hydromagnetic Stability*. Oxford University Press.

DEARDORFF, J. W. 1964 A numerical study of two-dimensional parallel-plate convection. *J. Atmos. Sci.* **21**, 419–438.

GLOBE, S. & DROPKIN, D. 1958 Natural convection heat transfer in liquids confined by two horizontal plates and heated from below. 1958 *Heat Trans. & Fluid Mech. Inst.* pp. 156–165. Berkeley, University of California.

HERRING, J. R. 1964 Investigation of problems in thermal convection: rigid boundaries. *J. Meteor.* **21**, 277–290.

KRUEGER, A. F. & FRITZ, S. 1961 Cellular cloud patterns revealed by Tiros I. *Tellus*, **13**, 1–7.

KUO, H. L. 1961 Solution of the non-linear equations of cellular convection and heat transport. *J. Fluid Mech.* **10**, 611–634.

MALKUS, W. V. R. 1954*a* Discrete transitions in turbulent convection. *Proc. Roy. Soc.* A, **225**, 185–195.

MALKUS, W. V. R. 1954*b* The heat transport and spectrum of thermal turbulence. *Proc. Roy. Soc.* A, **225**, 196–212.

NAKAGAWA, Y. & FRENZEN, P. 1955 A theoretical and experimental study of cellular convection in rotating fluids. *Tellus*, **7**, 1–21.

SILVESTON, P. L. 1958 Wärmedurchgang in Waagerechte Flüssigkeitsschichten. *Forsch. Ing. Wes.* **24**, 59–69.

THOMAS, D. B. & TOWNSEND, A. A. 1957 Turbulent convection over a heated horizontal surface. *J. Fluid Mech.* **2**, 473–492.